

# Vector Area Theorem mapping in crystals and polarization stability of SIT-solitons

V. N. Lisin<sup>1)</sup>

Kazan Physical-Technical Institute RAS, 420029 Kazan, Russia

Submitted 16 July 2001

Resubmitted 8 August 2001

The stability of polarization, areas, and number of self-induced transparency (SIT)-solitons at the output from the  $\text{LaF}_3 : \text{Pr}^{3+}$  crystal is theoretically studied versus the polarization direction and the area of the input linearly polarized laser pulse. For this purpose the Vector Area Theorem is rederived and two-dimensional Vector Area Theorem map is obtained. The map is governed by the crystal symmetry and takes into account directions of the dipole matrix element vectors of the different site subgroups of optically excited ions. The Vector Area Theorem mapping of the time evolution of the laser pulse allows one to highlight soliton polarization properties.

PACS: 42.50.-p, 42.65.-k, 78.20.-e

For an isotropic medium stability properties of self-induced transparency (SIT)-solitons are determined by the Area Theorem. The Area Theorem is the name given to a theoretical result that governs the coherent nonlinear transmission of short light pulses through isotropic materials, effectively two-level media, that have an absorption resonance very near the frequency of the incident light. In 1967 McCall and Hahn [1] identified a new parameter (called “Area” and denoted by  $\theta$ ) of optical pulses travelling in such media, and then predicted that the Area obeys the simple equation

$$\frac{\partial \theta}{\partial z} = -\frac{\alpha}{2} \sin \theta, \quad (1)$$

where  $\alpha$  is the attenuation coefficient for the material. The two most striking consequences of the Area Theorem are: (i) pulses with special values of Area, namely all integer multiples of  $\pi$ , are predicted to maintain the same Area during propagation, and (ii) pulses with other values of Area must change in propagation until their Area reaches one of the special values. This property can be shown to be unstable for the odd multiples, but the even multiples enjoy the full immunity of the theorem. The Eq.(1) was derived for the isotropic material in which the dipole matrix element vector of any ion is parallel to the electrical field vector of the light pulse. On the contrary, the direction of the dipole matrix element vector of any  $\text{Pr}^{3+}$  ion in  $\text{LaF}_3$  does not depend on the electrical field vector of the light pulse. So it is necessary to rederive Area Theorem taking into account directions of the dipole matrix element vectors of the

different subgroups of  $\text{Pr}^{3+}$  ions.  $\text{Pr}^{3+}$  ions in a  $\text{LaF}_3$  unit cell can replace  $\text{La}^{3+}$  in six different types of sites  $(\pm\alpha, \pm\beta, \pm\gamma)$ . The local environment of any of them has  $C_2$ -symmetry. The six local  $C_2$ -symmetry axes are located in the plane normal to the  $C_3$  axis and make the angle of  $2\pi/6$  in this plane (Fig.1). The electrical dipole

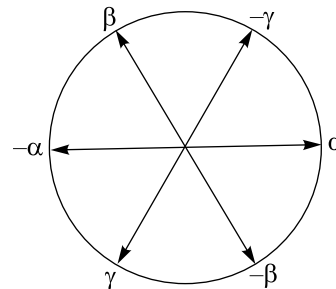


Fig.1. Directions of the local  $C_2$ -symmetry axes for the different  $\text{Pr}^{3+}$  ion sites in the plane normal to the  $C_3$ -axis of the  $\text{LaF}_3 : \text{Pr}^{3+}$  crystal.

matrix element vector of the  $\text{Pr}^{3+}$  ion (optical transition  $\Gamma_1 \rightarrow \Gamma_1$ )

$$\mathbf{p}_j = p\mathbf{e}_j, \dots j = 1, \dots, 6 \quad (2)$$

is directed [2] along the local  $C_2$  symmetry axis

$$\mathbf{e}_j = (\cos(j\frac{2\pi}{6}), \sin(j\frac{2\pi}{6})), \quad \mathbf{e}_z \cdot \mathbf{e}_j = 0, \quad (3)$$

where  $\mathbf{e}_j$  is the unit vector along the  $C_{2j}$  axis. Here the axis  $Z$  is directed along the  $C_3$  axis and the axis  $X$  along the  $\alpha$  axis. We define the Vector Area of the light pulse as

$$\Theta = \frac{p}{\hbar} \int_{-\infty}^{+\infty} dt \mathbf{E}(z, t), \quad (4)$$

<sup>1)</sup>e-mail: vlisin@kfti.knc.ru

where  $\mathbf{E}(z, t)$  is vector amplitude of the light pulse,  $p$  is electrical dipole matrix element,  $\hbar$  is the Planck constant. Taking into account Eqs.(2) and (3) and using arguments [3] we can write the equation for the Vector Area as follows:

$$\frac{\partial \Theta}{\partial z} = -\alpha \frac{1}{6} \sum_{j=1}^6 \mathbf{e}_j \sin(\Theta \cdot \mathbf{e}_j), \quad (5)$$

if a light pulse propagates along the  $C_3$ -axis. Here  $\alpha$  is the linear attenuation coefficient for  $\text{LaF}_3 : \text{Pr}^{3+}$ . As  $\Theta \rightarrow 0$ , Eq.(5) transforms to

$$\frac{\partial \Theta}{\partial z} = -\frac{\alpha}{2} \Theta, \quad (6)$$

as expected for a small pulse Area.

Equating the right-hand side of the equation (5) to zero we can find special values of the Vector Area where  $\partial \Theta / \partial z = 0$ . It can be made more obviously and easily from the graphical representation. We can rewrite eq. (5) as

$$\frac{\partial \Theta}{\partial z} = \frac{\partial}{\partial \Theta} \frac{\alpha}{6} \sum_{j=1}^6 \cos(\Theta \cdot \mathbf{e}_j) \quad (7)$$

and the problem is reduced to a determination of points in a two-dimensional plane, in which the function  $\sum \cos(\Theta \cdot \mathbf{e}_j)$  has extremes. The circles and triangles in Fig.2 give the contour plot of this function. We easily find three types of special values of the Vector Area, namely

$$\Theta_c = m\Theta_+ + n\Theta_-, \quad (8)$$

$$\Theta_u = \Theta_c + \mathbf{u}_j, \quad (9)$$

$$\Theta_s = \Theta_c + \mathbf{s}_j, \quad (10)$$

which are predicted to maintain the same Vector Area during propagation. Here  $m$  and  $n$  are arbitrary integers and

$$\Theta_+ = \frac{2\pi}{\cos(\pi/6)} \mathbf{k}_1, \quad \Theta_- = \frac{2\pi}{\cos(\pi/6)} \mathbf{k}_6; \quad (11)$$

$$\mathbf{s}_j = \frac{\pi}{\cos(\pi/6)} \mathbf{k}_j, \quad (12)$$

$$\mathbf{u}_j = \frac{\pi}{\cos^2(\pi/6)} \mathbf{e}_j, \quad (13)$$

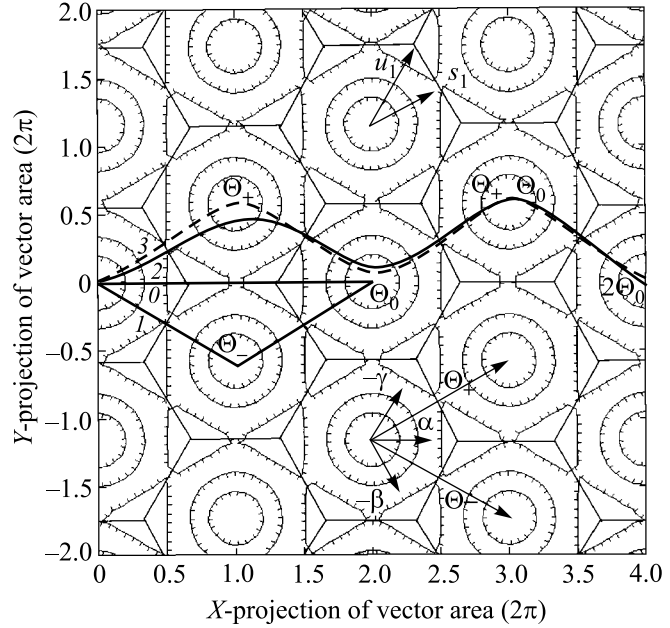


Fig.2. Vector Area Theorem map. The  $\Theta/2\pi$  projections to axes  $X$  and  $Y$  are plotted on axes  $X$  and  $Y$  accordingly. The vectors  $\mathbf{s}_1$  (12) and  $\mathbf{u}_1$  (13) are shown in the upper part of the figure. There are the basis vectors  $\Theta_+$  and  $\Theta_-$  (11) and the unit vectors along the local  $C_2$  symmetry axes ( $+\alpha, -\beta, -\gamma$ ) in the lower part of the figure. Vector coordinates of some unit cell centers are also shown. Bold lines 0 and 1 are mappings of the time evolution of laser pulses with  $\text{mod}(\Theta_0) = 4\pi$  and the angles between the directions of the Vector Area and the crystallographic axis  $\alpha$  are 0 and  $-1$  degrees respectively. In this case  $\alpha L = 20$ , where  $L$  is the sample length and  $\alpha$  is the attenuation coefficient. The bold line 2 is the mapping of the time evolution of the laser pulse with  $\text{mod}(2\Theta_0) = 8\pi$  and the angle between the directions of the Vector Area and the crystallographic axis  $\alpha$  is  $+1$  degree and  $\alpha L = 40$ . The bold line 3 is as 2 but  $\alpha L = 80$

where the unit vectors  $\mathbf{e}_j$  (3) and  $\mathbf{k}_j$  are directed respectively along and between the  $C_2$  axes:

$$\mathbf{k}_j = \left( \cos\left(j\frac{2\pi}{6} - \frac{\pi}{6}\right), \sin\left(j\frac{2\pi}{6} - \frac{\pi}{6}\right) \right). \quad (14)$$

These special points (8)–(10) give rise to a two-dimensional lattice in a  $\Theta$ -phase plane with basis vectors  $\Theta_+$  and  $\Theta_-$  (11) as it is shown in Fig.2. A unit cell of the lattice is determined by symmetry of the crystal. It is a regular hexagon. The hexagon centers are  $\Theta_c$  (8) (centers of the circles in Fig.2). As measured from the hexagon center, coordinates of the six apices of the hexagon are  $\mathbf{u}_j$  (13) (centers of the triangles in Fig.2), coordinates of middles of the sides of a hexagon are  $\mathbf{s}_j$  (12). It is obvious from Eqs.(5), (7) and definitions (8)–

(10), that in a neighborhood of these special points the Vector Area behaves as

$$\frac{\partial \Theta}{\partial z} = -\frac{\alpha}{2}(\Theta - \Theta_c), \quad (15)$$

$$\frac{\partial \Theta}{\partial z} = \frac{\alpha}{4}(\Theta - \Theta_u), \quad (16)$$

and as

$$\frac{\partial \Theta}{\partial z} = -\frac{\alpha}{6}(\Theta - \Theta_s), \quad (17)$$

if  $\Theta - \Theta_s$  is directed along the side of a hexagon, and

$$\frac{\partial \Theta}{\partial z} = +\frac{\alpha}{2}(\Theta - \Theta_s), \quad (18)$$

if  $\Theta - \Theta_s$  is directed perpendicularly to the side of a hexagon. Therefore, for an absorbing (amplifying) medium with  $\alpha > 0$  ( $\alpha < 0$ ), the points (8) are of the type of a stable (unstable) knot, the points (9) are of the type of an unstable (stable) knot and the points (10) are of the type of a saddle in the  $\Theta$ -phase plane. Below we shall explore a case of the absorbing medium with  $\alpha > 0$ . If the input pulse Vector Area falls inside the unit cell then the Vector Area must change in propagation until it reaches the unit cell center. If the input Vector Area does not equal to (9), (10) and falls on a side of a hexagon then the Vector Area must change in propagation until it reaches the middle of the hexagon side. It is necessary to note that the Vector Area Theorem map (Fig.2) allows us to easily predict only the sum of the pulse vector areas at the output from the sample. To determine the number of the output SIT-solitons and their polarization and area we should solve the system of coupled Maxwell-Bloch equations.

The input pulse with the Vector Area directed between the crystallographic axes and equal, for example, to  $\Theta_+$ , excites only four  $(\pm\alpha, \pm\gamma)$  ion subgroups. This pulse is  $2\pi$ -pulse for these ions. It does not excite  $\pm\beta$ -ions, because  $\Theta_+ \perp \mathbf{e}_{\pm\beta}$ . Similarly, the input pulse with the Vector Area equal to  $\Theta_-$  is the  $2\pi$ -pulse for  $(\pm\alpha, \pm\beta)$ -ion subgroups and does not excite  $\pm\gamma$ -ions. If the input Vector Area is parallel to the  $\Theta_+$  ( $\Theta_-$ ) and falls inside the unit cell  $\Theta_c = m\Theta_+$  ( $\Theta_c = m\Theta_-$ ), then the time evolution of the pulse may be described by the inverse scattering method. The input pulse is split at the output into  $m$  SIT-solitons with Vector Areas equal to  $\Theta_+$  ( $\Theta_-$ ), as in the isotropic medium. We refer to these solitons as  $\Theta_+$ -solitons and  $\Theta_-$ -solitons. If the input Vector Area is not parallel to the  $\Theta_+$  ( $\Theta_-$ ) but falls inside the unit cell  $\Theta_c = m\Theta_+$  ( $\Theta_c = m\Theta_-$ ), then

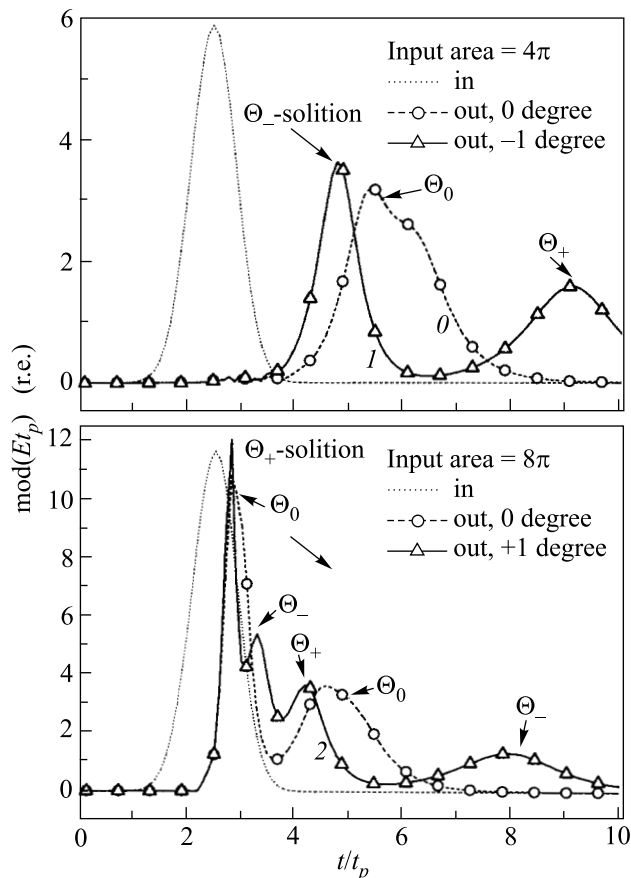


Fig.3. Time evolution of the amplitude of the laser pulses at the output of the sample. Values of the input Area, the angles between the directions of the Vector Area and the crystallographic axes  $\alpha$  and the parameter  $\alpha L$  for the curves 0, 1 and 2 are the same as for the curves 0, 1 and 2 in Fig.2. The parameter value  $\alpha L$  for the 0 degree curve in the lower part of the figure is the same as for curve 2. The dotted line is input pulse,  $t_p$  is input pulse duration. The Vector Area Theorem mapping (curves 1 and 2 in Fig.2) allows one to easily spot the polarizations and the areas of the solitons in the curves 1 and 2 in this figure

numerical calculations show that the input pulse also is split into  $m$   $\Theta_+$  ( $\Theta_-$ )-solitons at the output.

If the input pulse Vector Area is directed along the crystallographic axis, for example the axis  $\alpha$ , and is equal to

$$\Theta_0 = \Theta_+ + \Theta_-, \quad (19)$$

then all  $(\pm\alpha, \pm\beta, \pm\gamma)$  ions are excited. The input pulse is the  $2\pi$ -pulse for  $(\pm\beta, \pm\gamma)$  ion subgroups and the  $4\pi$ -pulse for  $(\pm\alpha)$  ions. The time evolution of the pulse is not described by the inverse scattering method. The numerical calculations show that if the input Vector Area  $\Theta_{in}$  is parallel to the  $\Theta_0$  and falls inside the

unit cell  $\Theta_c = m\Theta_0$ , then the input pulse is split into  $m$  SIT-solitons with Vector Areas equal to  $\Theta_0$ . We refer to these solitons as  $\Theta_0$ -solitons. Let the input Vector Area be not parallel to the  $\Theta_0$  and falls inside the unit cell  $\Theta_c = m\Theta_0$ . Then, as one can see in Figs.2, 3, a small change of the input pulse polarization leads to the splitting of each  $\Theta_0$ -soliton into  $\Theta_+$ - and  $\Theta_-$ -solitons. Therefore a number of solitons and their polarization strongly depend on the direction of the vector  $\Theta_{in}$  with respect to the crystallographic axis. This conclusion is also valid in the general case when the input Vector Area falls inside the unit cell  $\Theta_c = m\Theta_+ + n\Theta_-$ , where  $m \neq n$ . This is valid because the unit cell center coordinates may be rewritten as  $\Theta_c = (m - n)\Theta_+ + n\Theta_0$  if  $m > n$  or as  $\Theta_c = (n - m)\Theta_- + m\Theta_0$  if  $n > m$ . At first there are  $(m - n)\Theta_+$ -solitons for  $m > n$ , or  $(n - m)\Theta_-$ -solitons if  $n > m$  at the output. Then the number of solitons appearing at the output depends on the direction of the vector  $\Theta_{in} - (m - n)\Theta_+$  or  $\Theta_{in} - (n - m)\Theta_-$  with respect to the crystallographic axis. In the stable case the output solitons are  $\Theta_+$ -solitons and  $\Theta_-$ -solitons and their number is  $(m + n)$ .

For the amplifying medium  $\Theta_+$ -solitons and  $\Theta_-$ -solitons are unstable so the polarization of the output soli-

tons must be directed along crystallographic axis in the stable case.

It is necessary to note that for circular polarization of laser pulse the equation for the Area is of the form (1) as in the case of isotropic medium.

To summarize, we have shown on an example of the model system  $\text{LaF}_3 : \text{Pr}^{3+}$  that the Vector Area mapping of the pulse time evolution during propagation is an effective method to analyze the polarization properties of solitons.

We thank Ildar Ahmadullin for the help at assimilation of Fortran 90 and Ashat Basharov for the useful notes. The research was supported by ISTC grant # 737 and by the Russian Foundation for Basic Research grant # 00-02-16510.

- 
1. S. L. McCall and E. L. Hahn, Phys. Rev. Lett. **18**, 908 (1967).
  2. V. N. Lisin, Pis'ma v ZhETF **57**, 402 (1993) [JETP Lett. **57**, 415 (1993)].
  3. G. L. Lamb, in: *Elements of Soliton Theory*, John Wiley and Sons, New York, 1980.